# Second-harmonic generation in a near-field optical-fiber probe

**Tadashi Kawazoe**

*Exploratory Research for Advanced Technology, Japan Science and Technology Corporation, 687-1 Tsuruma, Machida, Tokyo 194-0004, Japan*

**Takashi Shimizu**

*Tokyo Institute of Technology, 4259 Nagatsuta, Midori-ku, Yokohama 226-8502, Japan*

**Motoichi Ohtsu**

*Exploratory Research for Advanced Technology, Japan Science and Technology Corporation, 687-1 Tsuruma, Machida, Tokyo 194-0004, Japan, and*
*Tokyo Institute of Technology, 4259 Nagatsuta, Midori-ku, Yokohama 226-8502, Japan*

Received July 5, 2001

Second-harmonic generation (SHG) in a near-field optical-fiber probe was observed. The tip of the probe consists of a triple-tapered fiber with an aluminum coating. For a fiber probe with an aperture size of 100 nm, the SHG conversion factor was $2.0 \times 10^{-11}$ cm$^2$/W, which is as large as that of a 5-mm KDP crystal. In a probe-to-probe experiment, we demonstrated that SHG took place at the aluminum coating on the fiber probe. © 2001 Optical Society of America

*OCIS codes:* 190.4370, 350.3950, 190.4350.

Near-field optics offers a unique technique for achieving high spatial resolution beyond the diffraction limit of light.[1] Various interesting kinds of study, such as spectroscopy of quantum dots[2] and polymers[3] and near-field (NF) optical chemical-vapor deposition,[4] have been carried out with this technique. Second-harmonic (SH) near-field optical imaging of a metal surface has also been reported.[5] Second-harmonic generation (SHG) is a useful phenomenon not only for far-field spectroscopy but also for NF spectroscopy, which one can use to investigate material properties and examine nonlinear optical devices. A SH signal is generated by nonlinear polarization involving the asymmetric property of the material. A fiber probe used for NF optics can satisfy this condition, because it has large asymmetric regions in the sharpened fiber core, coated metal, and air. In addition, the coated metal surface can enhance the SHG intensity as a result of the surface plasmon effect.[6] The SHG efficiency of an apertureless metallic tip has been reported, and it may not be so low as that of a nonlinear crystal.[7] For a metal-coated fiber probe with an aperture, the SHG efficiency may not be so low, because of the complicated profile of the boundary between glass and metal. However, we know of no investigation of SHG in a fiber probe, in spite of its potential application to frequency conversion, optical chemical-vapor deposition with UV light, and so on. Thus we believe that it is important to investigate the phenomenon of SHG in fiber probes. In this Letter we demonstrate SHG in a fiber probe and report several of its properties for the first time to our knowledge.

Figure 1(a) shows the cross-sectional profile and a scanning-electron microscope (SEM) image of the NF fiber probe employed for SHG. A triple-tapered fiber probe, configured for use in the UV region,[8] was used as the NF probe. The fiber had a double-core structure consisting of a 0.16-$\mu$m $GeO_2$-doped core and a 3.0-$\mu$m pure-silica sheath. In fabricating the probe we used two buffered hydrogen fluoride (BHF) solutions as etchants. The two solutions differed in their ratios of $NH_4F$ solution (40 wt. %):HF acid (50 wt. %):$H_2O$, which were 1.7:1:1 ($BHF_A$) and 10:1:1 ($BHF_B$). First, we etched the fiber end with $BHF_A$ for 56 min to taper the fiber. Next, we etched the tapered fiber with $BHF_B$ for 30 min to sharpen the center of the fiber core. The general shape of the probe was that of a cone with an angle of 17°. The triple-tapered end was coated with a 500-nm-thick aluminum layer by vacuum deposition. Two probes were prepared. We prepared probe A by coating the

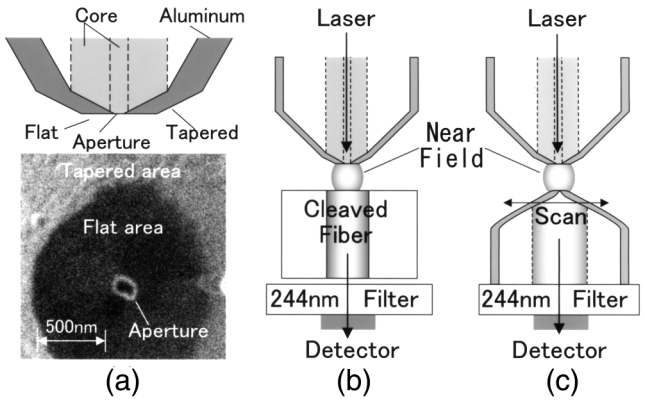


Fig. 1. Explanation of the experiments and the fiber probe. (a) Cross-sectional profile and a SEM image of the near-field probe for SHG. (b) Schematic drawing of the experimental configuration for measurement of SH intensity from the probe. (c) Schematic drawing of the probe-to-probe experiment.

0146-9592/01/211687-03$15.00/0 

aluminum from the top and probe B by coating it from the side. The probe apertures were created by use of the focused ion-beam technique. The roughness of the cut end was less than 5 nm, which was the spatial resolution of the SEM. The diameter of the aperture was found from the SEM image to be 100 nm.

Figure 1(b) is a schematic drawing of the experimental setup for measuring SH intensity. The SH intensity was measured with a cleaved fiber. The 10-$\mu$m core of the cleaved fiber was much larger than the apex diameter of the probe, and the distance between the cleaved fiber and the probe was less than 1 $\mu$m. Therefore, most of the fundamental and SH signals from the probe could be detected by the cleaved fiber. Figure 1(c) explains the method used for measuring the spatial distribution of the SH intensity in the probe-to-probe experiment.[9] The second probe used in the probe-to-probe scanning was a single tapered fiber probe that was fabricated by pulling and etching of a fiber with a pure silica core that was then coated with a 500-nm-thick layer of aluminum.[10] The diameter of its aperture was 100 nm. Separation between the two probes was regulated to several nanometers by use of a shear-force technique.[11] A 488-nm-wavelength $Ar^+$ laser was used as the light source for the experiments. We used a Hamamatsu Model R166UH photomultiplier tube, because it is sensitive in the wavelength range 160–320 nm, to detect the SH signal selectively. In addition, we used a bandpass filter with a bandwidth of 10 nm to reject the fundamental signal with an extinction ratio higher than $10^{-4}$ for the fundamental wavelength. The quantum efficiency of the photomultiplier tube was more than 30% for 244-nm light. A photon-counting technique was used for detection. For an accumulation time of 1000 s, the lowest observable SH power was $3.0 \times 10^{-19}$ W.

Figure 2 shows the relationship between the fundamental and the SH powers when we used the fundamental signal passing through the probe as the reference for this measurement. The squares correspond to the experimental results for probe A. The SHG power is proportional to the square of the fundamental power in the low-power region and saturates at a fundamental power of ~20 nW. As the fiber probe can be thermally damaged by a fundamental output exceeding 100 nW, the observed saturation at 20 nW is reasonable. Thermal damage changes properties of the fiber probe such as aperture diameter and aluminum coating; then the SH signal intensity is saturated. The solid line in Fig. 2 fits the measured values in the unsaturated region. The conversion factor $R$ is the ratio of the SH intensity to the square of the fundamental intensity. From the slope of the solid line, the value of $R$ for probe A with an aperture of 100 nm is $2.0 \times 10^{-11}$ cm$^2$/W. Because this value depends on the aluminum deposition technique, SHG was also evaluated for probe B, which was fabricated by the alternative approach of depositing aluminum from the side of the triple-tapered fiber. The results are shown by filled circles in Fig. 2, and the dashed line fits the data points for probe B in the unsaturated region. The slope of this line gives the $R$ value for probe B, which is estimated to be $2.1 \times 10^{-12}$ cm$^2$/W, i.e., ten times smaller than the value for probe A. Such a large difference in the value of $R$ supports the dependence of SHG on the deposition technique. Furthermore, it should be noted that the values of $R$ for probes A and B are 5 orders of magnitude higher than that obtained for an aluminum surface coated upon a large flat piece of glass.[12] Such a large value corresponds to the value for a 5-mm-thick KDP crystal in the far-field configuration.[13] We believe that the highly efficient SHG localized at a small probe has immense potential for a wide range of applications.

Figure 3(a) shows the spatial distribution of the SH power on probe A obtained in the probe-to-probe experiment. The image size is 1.5 $\mu$m × 1.5 $\mu$m. The solid ellipse (X) shows the position of the aperture, and the dashed curve (Y) shows the boundary between the flat and the tapered areas. Strong SH light is emitted at the areas enclosed by the dotted dumbbell curve and about the boundary (Y). Figure 3(b) shows cross-sectional profiles of the SH power along the solid and

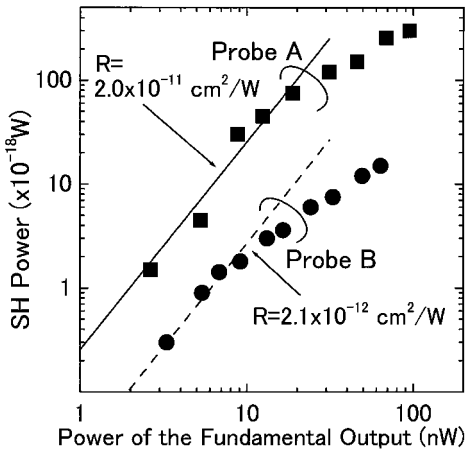


Fig. 2. Relation between the fundamental and the SH powers. Squares and circles represent the experimental results with probes A and B, respectively; the solid and dashed lines are fitted to them in the unsaturated region.

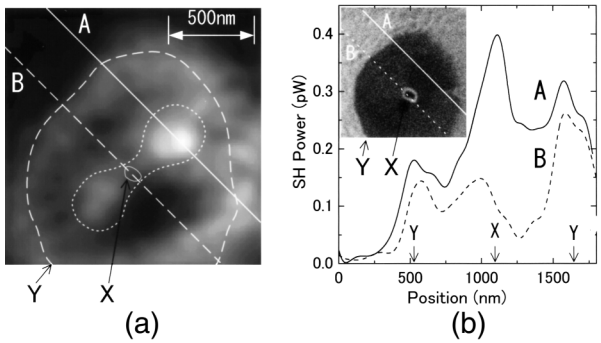


Fig. 3. Spatial distribution of the SH power on probe A measured by the probe-to-probe experiment. (a) Two-dimensional profile of SH distribution. Solid ellipse (X), position of the aperture. Dashed curve (Y), boundary between the flat and the tapered areas, as shown in Fig. 1(a). (b) Cross-sectional profiles of the distribution along A, the solid and B, the dashed lines marked in (a). Inset, SEM image of the probe corresponding to (a).

dashed lines in Fig. 3(a). The inset in Fig. 3(b) shows a top-view SEM image of the probe, and the image area corresponds to that of Fig. 3(a). The peak power of the SH signal was 0.4 pW. This observed power is much larger than the previous experimental result, shown in Fig. 2. We believe that this enhancement of SH signal comes from the resonant effect of two probes. In the area enclosed by the dotted dumbbell curve, a strong SH signal was recorded from both sides of the aperture. The SHG observations within the area enclosed by the dumbbell curve may be related to polarization of the SH light and correspond to the propagation mode of the fiber.[10] Near the boundary between the flat and the tapered areas (Y), nonlinear oscillation of the surface plasmon in the aluminum coating could easily emit SH light as a result of the edge effect. These results confirm that the SH signal was generated in the aluminum coating. Investigations of SHG in a bare-fiber probe without aluminum coating revealed no detectable SH signals despite a high fundamental intensity. This result also strongly indicates that the aluminum coating enhances SHG in the fiber probe. In a subwavelength-sized fiber probe, the optical NF becomes dominant and can excite the surface plasmon polariton on the coated metal, an effect that is well known in the case of flat metal surfaces.[6] Therefore we believe that the SHG enhancement with the fiber probe occurs as a result of the optical nonlinear response of the surface plasmon polaritons on the coated metal.

In conclusion, we have demonstrated SHG in a near-field optical-fiber probe for what we believe is the first time. A high SHG conversion factor in the range $2.1 \times 10^{-12}$–$2.0 \times 10^{-11}$ $cm^2/W$ was obtained for a 100-nm-aperture fiber probe. This highly efficient SHG promises several new applications in NF optics. The spatial distribution of SHG on the fiber probe was determined in a probe-to-probe experiment. The experimental results establish that the aluminum coating on the fiber probe and the shape of the fiber probe are important factors that govern this SHG phenomenon. Further studies to clarify the mechanism by which this SHG occurs would be useful.

T. Kawazoe's e-mail address is kawazoe@ohtsu.jst.go.jp.

## References

1. D. W. Pohl and D. Courijon, eds., *Near Field Optics* (Kluwer Academic, Dordrecht, The Netherlands, 1993).
2. T. Matsumoto, M. Ohtsu, K. Matsuda, T. Saiki, H. Saito, and K. Nishi, Appl. Phys. Lett. **75,** 3246 (1999).
3. R. Stevenson, M. Granstrom, and D. Richards, Appl. Phys. Lett. **75,** 1574 (1999).
4. Y. Yamamoto, M. Kourogi, M. Ohtsu, V. Polonski, and G. H. Lee, Appl. Phys. Lett. **76,** 2173 (2000).
5. I. I. Smolyaninov, A. V. Zayats, and C. C. Davis, Phys. Rev. B **56,** 9290 (1997).
6. V. M. Agranovich and D. L. Mills, ed., *Surface Polaritons: Electromagnetic Waves at Surfaces and Interfaces* (North-Holland, Amsterdam, 1982).
7. I. I. Smolyaninov, H. Y. Liang, C. H. Lee, C. C. Davis, S. Aggarwal, and R. Ramesh, Opt. Lett. **25,** 835 (2000).
8. S. Mononobe, T. Saiki, T. Suzuki, S. Koshihara, and M. Ohtsu, Opt. Commun. **146,** 45 (1998).
9. T. Yatsui, M. Kourogi, and M. Ohtsu, Appl. Phys. Lett. **71,** 1756 (1997).
10. M. Ohtsu, ed., *Near-Field Nano/Atom Optics and Technology* (Springer-Verlag, Berlin, 1998).
11. E. Betzig, P. L. Finn, and J. S. Weiner, Appl. Phys. Lett. **60,** 2484 (1992).
12. R. Murphy, M. Yeganeh, K. J. Song, and E. W. Plummer, Phys. Rev. Lett. **63,** 318 (1989).
13. A. Yariv, *Introduction to Optical Electronics*, 3rd ed. (Holt, Rinehart, & Winston, New York, 1985).